

Functionalized scaffolds of shorter self-assembling peptides containing MMP-2 cleavable motif promote fibroblast proliferation and significantly accelerate 3-D cell migration independent of scaffold stiffness†‡§

Yoshiyuki Kumada,^{ab} Nathan A. Hammond^a and Shuguang Zhang^{*a}

Received 6th May 2010, Accepted 28th June 2010

DOI: 10.1039/c0sm00333f

The functionalization of self-assembling peptide scaffolds with biologically active motifs presents many possibilities for the design of synthetic biological materials for 3D cell culture, reparative, regenerative medicine and tissue engineering. We here report the development of short self-assembling peptide scaffolds designed especially for cell migration. We designed self-assembling peptide scaffolds VEVK9 (Ac-VEVKVEVKV-CONH₂) and VEVK12 (Ac-VEVKVEVKVEVK-CONH₂) and modified variants of these peptides directly coupled to short biologically active motifs. These motifs include two-unit RGD binding units (PRGDSGYRGDS), cell adhesion sequences of laminin (YIGSR and IKVAV) and a Matrix metalloproteinase-2 (MMP-2) cleavable sequence (PVGLIG). We show here that the peptide scaffolds functionalized with these cell adhesion motifs significantly promoted proliferation of periodontal ligament fibroblasts. Moreover, when combined with the MMP-2 cleavable motifs, the peptide scaffolds significantly accelerated the fibroblasts' migration independent of scaffold stiffness. Our results suggest that the interaction between integrin receptors of fibroblasts and cell adhesion motifs of the scaffolds stimulated MMP-2 production from the fibroblasts to accelerate proteolytic cell migration in the similar manner as natural extracellular matrix. These peptide scaffolds may be useful in tissue engineering and regenerative medicine including periodontal tissue reconstruction.

1. Introduction

We previously reported the discovery and development of a class of self-assembling peptides made of only natural amino acids. This class of material peptides can undergo spontaneous assembly into well-ordered nanofibers and scaffolds, ~10 nm in fiber diameter with pores between ~5–200 nm in diameters and over 99% water content.^{1,2} These peptide scaffolds have three-dimensional nanofiber structures similar to natural extracellular matrix including collagen. They serve as a convenient platform for developing new designs of biomimetic synthetic extracellular matrix.^{2–5}

One family of these peptide scaffolds, RADA16-I(Ac-RADARADARADARADA-CONH₂) and its functionalized peptide scaffolds have shown great promises in bone, cartilage, and neural regeneration, to instantly stop bleeding as well as for slow and sustained molecular release.^{6–10} The self-assembling peptide can be easily functionalized with biologically functional peptide motifs to promote a specific cellular response. However,

functionalization of self-assembling peptides can result in a long peptide sequence, which is complex and expensive to manufacture. Also, cells respond favorably to culture on scaffolds with low peptide concentration, yet at these concentrations the peptide scaffold becomes very weak and difficult to handle for cell culture or clinical use. Therefore, there remains a need for a peptide scaffold that is inexpensive, easy to use, and effective for cell culture.

It is known that the formation of self-assembling peptide scaffold and its mechanical properties are influenced by several factors, one of which is the level of hydrophobicity.^{11–16} That is, in addition to the ionic complementary interactions, the extent of the hydrophobic residues, Ala, Val, Ile, Leu, Tyr, Phe, Trp (or single letter code, A, V, I, L, Y, F, W) can significantly influence the mechanical properties of the scaffolds and the speed of their self-assembly. Higher hydrophobicity corresponds to a shorter length of peptide required for self-assembly, easier scaffold formation, and better mechanical properties. However, this property does not necessarily promote cell migration, so additional active motifs may be needed to stimulate cell adhesion.

Adhesion between cells and the matrix is very important for cell growth. The functionalization of peptide scaffold with cell adhesion motifs RGD (Arg-Gly-Asp) and cell adhesion motifs from laminin has been shown to be effective in increasing cell proliferation, migration and differentiation.^{8,9}

Recently, peptides that are sensitive to the enzymatic cleavage of matrix metalloproteinases (MMPs) have been added to synthetic polymers and peptide-amphiphiles.^{17–24} MMPs belong to a family of proteases that degrade extracellular matrix components and therefore play important roles in tissue

^aCenter for Biomedical Engineering, Massachusetts Institute of Technology, 77 Massachusetts Avenue, Cambridge, MA, 02139, USA. E-mail: shuguang@mit.edu

^bOlympus America Inc., 3500 Corporate Parkway, Center Valley, PA, 18034, USA

† This paper is part of a joint *Soft Matter* and *Journal of Materials Chemistry* themed issue on Tissue Engineering. Guest editors: Molly Stevens and Ali Khademhosseini.

‡ Electronic supplementary information (ESI) available: Further 3-D confocal microscopy images. See DOI: 10.1039/c0sm00333f

§ Designed and performed the experiments except AFM experiments: S.Z. and Y.K. Performed AFM experiments: N.H. Wrote the paper: S.Z. Y.K.

regeneration. They make space in the matrix for cells to expand and migrate, enabling extracellular matrix remodeling and tissue growth. In addition to cell adhesion motifs, incorporating MMP-cleavable substrates into self-assembling peptide scaffolds is an attractive strategy to engineer a dynamic mechanism for eliciting remodeling activities in cells and tissue.

We here report the design of the two self-assembling peptides VEVK9 (Ac-VEVKVEVKV-CONH₂), and VEVK12 (Ac-VEVKVEVKVEVK-CONH₂) and the functionalization of VEVK9 by synthesizing extended sequences with a designed 2-unit RGD binding sequence (PRGDSGYRGDS) or one of two cell adhesion motifs derived from laminin (YIGSR, IKVAV) added at the C-terminus. The designed 2-unit RGD sequence has previously been shown to be effective in osteoblasts and endothelial cell growth.^{8,25} The self-assembling peptide VEVK9 has only 9 amino acid residues and its functionalized peptides are shorter than those of RADA16-I, which has 16-amino acid residues, and VEVK9 has the potential for promoting cell activities in a similar way.

We also report the functionalization of VEVK9 with an MMP-2 cleavable sequence. We inserted an MMP-2 cleavable sequence (PVGLIG) into the self-assembling peptide VEVK9. This sequence was selected by screening a combinatorial peptide library for optimal MMP substrates.²⁶ The self-assembling peptide scaffold functionalized with this sequence, (RADA)₃ PVGLIG (RADA)₃, has been shown to be degradable by MMP-2, showing promise for use as a tissue engineering scaffold.¹⁹

We here showed that these functionalized peptide scaffolds significantly increased the proliferation of periodontal ligament fibroblasts in comparison to the non-functionalized peptide scaffolds VEVK9 and VEVK12. Moreover the peptide scaffolds functionalized with the MMP-2 cleavable sequence significantly promoted the fibroblasts migration. Our results suggest that these functionalized peptide scaffolds are less expensive and may be useful as scaffold materials with potential applications in areas such as tissue engineering and regenerative medicine.

2. Experimental

2.1 Peptide solution preparation and gel formation

All self-assembling and functionalized peptides tested here were custom-synthesized by CPC Scientific (Purity > 80%, San Jose, CA). They were dissolved in water at a final concentration of 1% (w/v, 10 mg/ml) and sonicated for 20 min (aquasonic, model 50T, VWR, NJ). After sonication, they were filter-sterilized (Acrodisc Syringe Filter, 0.2µmHT Tuffrun membrane, Pall Corp., Ann Arbor, MI) for later use. The functionalized peptide solutions vPRG, vYIG and vIKV were mixed in a volume ratio of 1 : 1 with non-functionalized peptide solution VEVK9 or VEVK12. The solution vPVG was mixed with the functionalized and non-functionalized peptide solutions above in a volume ratio of 1 : 1 : 2. The desired number of cell culture inserts (10mm diameter, 0.4 µm pore size, BD Bioscience, Bedford, MA) were placed in a 24-well culture plate with 250µl culture medium in each well. 100 µl peptide solution was loaded directly into each of the inserts and then incubated for at least 1 h at 37 °C for gelation. 100 µl of culture medium was added onto the gel and then incubated overnight at 37 °C. Once the gel was formed, the

medium was removed and changed twice more to equilibrate the gel to physiological pH prior to plating the cells.

2.2 Cell culture of periodontal ligament fibroblasts

Primary isolated human periodontal ligament fibroblasts were commercially obtained from Lonza Inc. (HPDLF, Walkersville, MD) and routinely grown in the culture medium (SCGM, Walkersville, MD) on ordinary cell culture flasks. The cells were plated at 2×10^4 cells on the gel in the inserts. The culture medium was changed every three days.

2.3 Fluorescence microscopy

Following the experiments, the cells on the gel were fixed with 4% paraformaldehyde for 15 min and permeabilized with 0.1% Triton X-100 for 5 min at room temperature. Fluorescent Rhodamin phalloidin and SYTOX® Green (Molecular Probes, Eugene, OR) were used for labeling F-actin and nuclei, respectively. Images were taken using a laser confocal scanning microscope (Olympus FV300). Cell numbers were counted in three random fields per substrate with the aid of the microscope above with a 10× objective. Cell densities were then calculated using the numbers of counted cells and the magnifying power of the microscope. Cell migration depths were estimated based on vertical scanning range of the microscope.

2.4 Structural study with atomic force microscopy (AFM)

Peptide filaments imaging. Peptide solution was diluted to 0.01 mg/ml in 0.01 M HCl. The diluted solution was shaken vigorously for 20 s before 5 µl peptide solution was pipetted onto a freshly cleaved mica surface. After 20 s, the mica was rinsed with 500 µl of deionized water and wicked dry with tissue paper. Peptide solutions were allowed to dry and were scanned within 24 h using a Nascatec (Kassel, Germany) model NST-FM probe (70 kHz) on a Veeco Nanoscope IIIa Multimode atomic force microscope (Plainview, NY) in tapping mode.

Peptide stiffness measurement. Washer-shaped molds were made from a 1.1 mm sheet of polycarbonate plastic using circular punches (inner diameter 3.2 mm, outer 11 mm). To contain peptide while allowing diffusion of PBS from outside, a piece of backing paper (nitrocellulose membrane, Pall LifeSciences, Port Washington, NY) was affixed to one side of each mold with high-vacuum grease (Dow Corning, Midland, MI). The mold was placed in a 35 mm culture dish (BD Biosciences, San Jose, CA) with the paper downward on a piece of Kimwipe tissue (Kimberly Clark, Irving, TX) soaked with Dulbecco's PBS (Lonza Biowhittaker, Walkersville, MD). The mold was then filled with 12 µl of peptide solution freshly sonicated (Sonics Vibra-Cell, Newtown, CT) at 50% power for 90 s, and the culture dish was closed and sealed with Parafilm M (Pechiney Plastics Packaging, Menasha, WI). One hour later the dish was opened, the gel was covered with PBS, and the dish was again sealed. 24 h were allowed before taking measurements by indentation.

AFM tips for microindentation were prepared by gluing one 10-µm polystyrene bead (Polysciences, Warrington, PA) near the tip of each AFM cantilever (model TR400PSA, 80 pN/nm, Asylum Research, Santa Barbara, CA) with Loctite 3211 light

cure adhesive (Henkel, Dusseldorf, Germany) and placing under an ultraviolet lamp (Raytech Industries, Middletown, CT) for 1 h. Tips were calibrated in PBS on an MFP-3D atomic force microscope (Asylum Research) using the thermal calibration method,²⁷ giving tip stiffness values between 80 and 105 pN/nm. Measurements were collected from triplicate samples of each gel type. A force-indentation curve was collected from 20 random points on each gel by bringing the tip in contact with the gel at a rate of 5 $\mu\text{m/s}$ up to a trigger force of 10 nN before retracting.

The relationship between force and indentation depth for a rigid sphere impacting an ideal elastic solid is given by the Hertz model in eqn (1), where F is force, E is Young's modulus, ν is the Poisson ratio, R is the radius of the sphere, and δ is the indentation depth into the material. To obtain Young's modulus from the force-indentation data, an in-house MATLAB script was used to find a least-squares fit of the Hertz model (eqn (1)) to the approach curve by varying the force and displacement offsets (values of F and δ taken as 0) and the Young's modulus E . The bead radius is 5 μm , and Poisson's ratio ν is taken as 0.5.

$$F = \frac{4E}{3(1-\nu^2)} R^{\frac{1}{2}} \delta^{\frac{3}{2}} \quad (\text{Eqn 1})$$

2.5 Statistical analysis

The mean values are presented with standard deviations (SDs). Student's *t*-test for unpaired samples was used to calculate the significance of difference in the mean values. A value of $P < 0.01$ or 0.05 was considered to be statistically significant.

3. Results and discussion

3.1 Synthesis of self-assembling peptides

The peptide sequences and descriptions are listed in Table 1. VEVK9 and VEVK12 are simple repeating units of amino acids VEVK (Valine-Glutamate-Valine-Lysine) which self-assemble into a nanofiber structure. The self-assembling peptide VEVK9 was functionalized either with RGD, laminin cell adhesion motifs or an MMP-2 cleavable motif in order to mimic extracellular matrix to enhance cell maintenance and function in cell cultures. The functionalized peptides vPRG, vYIG and vIKV were synthesized with the VEVK9 sequence plus an additional motif added to the C-terminus using solid phase synthesis (Fig. 1a). One motif contains two repetitions of the RGD sequence (PRGDSGYRGDS), and the others are cell adhesion motifs of laminin (YIGSR, IKVAV). Glycine residues were used between the self-assembling motif VEVKVEVKV and the functional motif as a spaced linker to keep the flexibility of the functional peptides. The MMP-2 cleavable motif (PVGLIG) was

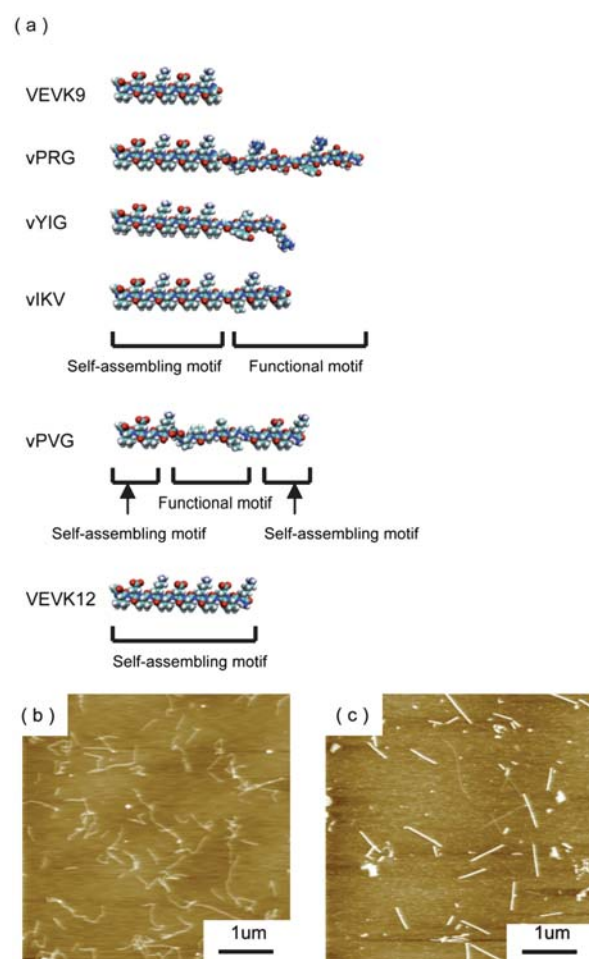


Fig. 1 (a) Molecular models of designer peptide VEVK9, vPRG, vYIG, vIKV, vPVG and VEVK12 and AFM images of peptide solutions, (b) VEVK12, (c) VEVK9 mixed with vPRG and vPVG. These AFM images show nanofiber formation. The bar represents 1 μm .

inserted between two VEVK units (Fig. 1a). In comparison to RADA16-I and its functionalized peptides, these peptides are short sequences, maximum 20 amino acids (in vPRG), and seem to be cost-effective. The peptides were solubilized in water at a concentration of 10 mg/ml (1%, w/v). They readily undergo self-assembly to form scaffold hydrogels. Mixing with self-assembling peptide VEVK9 or VEVK12 facilitated self-assembly and gelation. Tapping mode AFM was used to analyze the formation of nanofibers because this system allowed us to observe peptide nanofiber structure without damaging them. Fig. 1b-c show clearly that the self-assembling peptides VEVK12

Table 1 Designer self-assembling peptides used in this study

Name	Sequence	Description
VEVK9	Ac-VEVKVEVKV-NH ₂	Designer self-assembling motif
vPRG	Ac-VEVKVEVKV- GPRGDSGYRGDS-NH ₂	2-unit RGD motifs
vYIG	Ac-VEVKVEVKV-GYIGSR-NH ₂	Laminin cell adhesion domain (YIGSR)
vIKV	Ac-VEVKVEVKV-GIKVAV-NH ₂	Laminin cell adhesion domain (IKVAV)
vPVG	Ac-VEVK- GPVGLIG-VEVK-NH ₂	MMPs cleavage site (PVGLIG)
VEVK12	Ac-VEVKVEVKVEVK-NH ₂	Designer self-assembling motif

(Fig. 1b) and VEVK9 mixed with functionalized peptides vPRG and vPVG (Fig. 1c) formed nanofibers in aqueous solutions.

3.2 Cell adhesion on functionalized peptide scaffolds

In order to evaluate cell attachment on each peptide scaffold, the same number of cells were seeded on each scaffold and cultured for three weeks. Fig. 2 a–h show the typical morphologies of periodontal ligament fibroblasts on different scaffolds. The fibroblasts exhibited good attachment and extension on the peptide scaffolds functionalized with vPRG, vYIG and vIKV, particularly on VEVK9 mixed with vYIG (Fig. 2c) and vIKV (Fig. 2d). In contrast, on non-functionalized peptide scaffolds VEVK9 (Fig. 2a) and VEVK12 (Fig. 2e) cells are sparse and have a rounded morphology. Fig. 3 shows cell numbers on each scaffold after three weeks culture. It is clear that all functionalized peptides tested here significantly promoted cell proliferation, especially in scaffolds made with VEVK9.

It is known that periodontal ligament fibroblasts adhere to the RGD motif, fibronectin and laminin and express the integrin subunits related to the attachment to these extracellular matrix proteins.^{28,29} Thus, the inclusion of these cell adhesion motifs in the peptide scaffolds seems to promote the fibroblasts' adhesion, proliferation and 3-D migration through the interaction with integrin receptors of the fibroblasts. Interestingly, these results showed the differences in effectiveness of the functionalized motifs between the self-assembling peptides VEVK9 and VEVK12. Fig. 3 clearly demonstrates that the functionalized peptide motifs included in the peptide scaffold VEVK9 are more effective for cell proliferation than those in VEVK12. It has been reported that a functional motif physically incorporated into the nanofibers of a scaffold affects cell growth.⁸ It appeared in this study that the functionalized peptides are incorporated well in self-assembling peptide VEVK9 to form nanofibers with the

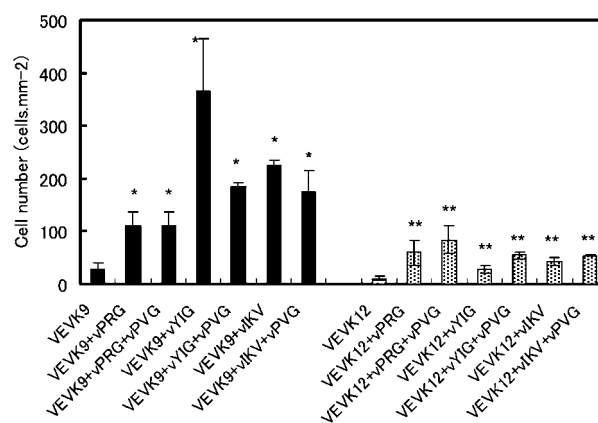


Fig. 3 Cell numbers on each peptide scaffold after three weeks culture. VEVK9 is 100% of non-functionalized peptide scaffold, VEVK9 + vPRG is non-functionalized peptide VEVK9 mixed with functionalized peptide vPRG in a volume ratio of 1 : 1. VEVK9 + vPRG + vPVG is non-functionalized peptide VEVK9 mixed with functionalized peptide vPRG and vPVG in a volume ratio of 2 : 1 : 1. Other labels follow the same pattern. Cell numbers on peptide scaffolds VEVK9 mixed with functionalized peptides are significantly higher than that on non-functionalized peptide scaffold VEVK9 (* $P < 0.01$ vs. VEVK9). Peptide scaffolds VEVK12 mixed with functionalized peptides follow a same pattern (** $P < 0.01$ vs. VEVK12).

functional motifs. In contrast, it is possible that the functionalized peptides interfere with the self-assembly process of VEVK12 due to distortion of the β -sheet structure formation. As a result, some of the functional motifs are not incorporated into the nanofibers and are unable to function. Further study regarding the interaction will be required. It also has been reported that stiffness of peptide scaffold affects cell adhesion.¹⁰ We will discuss the effect of stiffness of the scaffold on cell growth later.

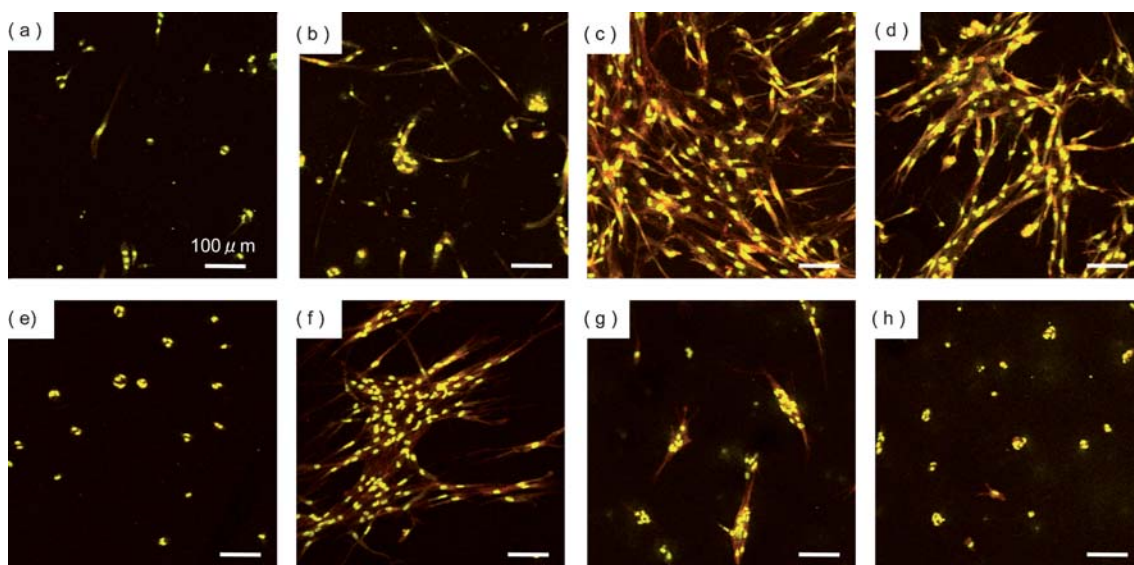


Fig. 2 Confocal microscopy images of periodontal ligament fibroblast morphology on peptide scaffold (a) VEVK9, (b) VEVK9 mixed with vPRG, (c) VEVK9 mixed with vYIG, (d) VEVK9 mixed with vIKV, (e) VEVK12, (f) VEVK12 mixed with vPRG, (g) VEVK12 mixed with vYIG and (h) VEVK12 mixed with vIKV. Fluorescent staining with Rhodamin phalloidin for F-actin (red) and SYTOX Green for nuclei (yellow) showed the cell attachments and distributions. The bar represents 100 μm .

3.3 Cell migration into functionalized peptide scaffolds

We previously showed that cells spontaneously migrate into the 3D scaffold using 3-D image collections and reconstructions obtained by confocal microscopy.⁸ We show the results in Fig. 4, the reconstructed images of periodontal ligament fibroblasts in the peptide scaffold VEVK9 (Fig. 4a), VEVK9 mixed with functionalized peptide vPRG alone (Fig. 4b), mixed with vPRG and vPVG (Fig. 4c), mixed with vYIG and vPVG (Fig. 4d), and mixed with vIKV and vPVG (Fig. 4e). Migrating cells were clearly discernible by confocal imaging and differences in the characteristics of these scaffolds were found. Only a few fibroblasts adhered to the peptide scaffold with VEVK9, and these remained near the surface (Fig. 4a). In peptide scaffolds with VEVK9 mixed with functionalized peptides, a large number of cells appeared on surface and inside of the scaffolds (Fig. 4b–e). Furthermore, we show in Fig. 5 that the fibroblasts initially attached to the surface of the scaffold at day 1 proliferated as well as migrated into the scaffold spontaneously. The images in Fig. 4a–c exhibit significant increases in fibroblast proliferation and migration due to the effects of the functionalized peptides vPRG and vPVG. It appears in Fig. 4c that the fibroblasts on the surface of the scaffold migrated into the scaffold to enlarge their sphere of activity.

It is known that periodontal ligament fibroblasts contribute greatly to the remodeling of periodontal tissue by secreting MMP-2 for degradation and synthesizing extracellular matrix proteins for replacement.³⁰ It is also known that MMP regulation occurs by integrin binding, for example by $\alpha_v\beta_3$, which is the main RGD-binding integrin.³¹ They suggest that the fibroblasts recognized the exposed RGD adhesion motifs of the scaffold *via* integrin receptors to adhere to the scaffold. The interaction between the integrin and the RGD motifs yields MMP-2 production by the fibroblasts. As a result, the fibroblasts moved deeper into the scaffold, breaking the MMP cleavable sites incorporated into the scaffold. Interestingly, in the case of VEVK9 mixed with only vPVG (without vPRG), the fibroblasts

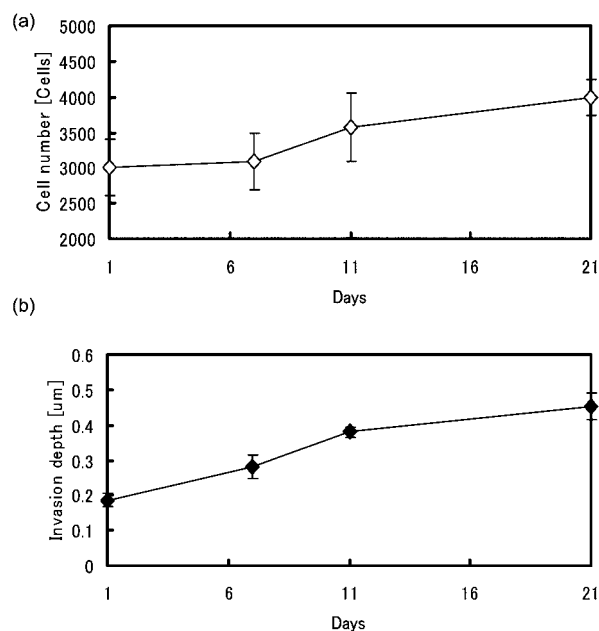


Fig. 5 Periodontal ligament fibroblasts growth in VEVK9 mixed with vPRG and vPVG. (a) Cell numbers and (b) invasion depths were measured after 1 day, 7 days, 11 days and 21 days culture. Migration depth was measured by 3-D confocal microscopy images of fibroblasts. Periodontal ligament fibroblasts proliferated as well as migrated into the scaffold spontaneously.

were rounded on surface of the scaffold and did not proliferate or migrate into the scaffold, which is similar to the case of VEVK9 (Fig. 4a). Thus, a cell adhesion motif which interacts with integrin seems to play an important role as a stimulus for proteolytic cell migration into the enzymatically degradable scaffold.²¹ In the case of scaffolds functionalized with laminin cell adhesion motifs vYIG and vIKV, the fibroblasts appear to migrate into them in the same manner.

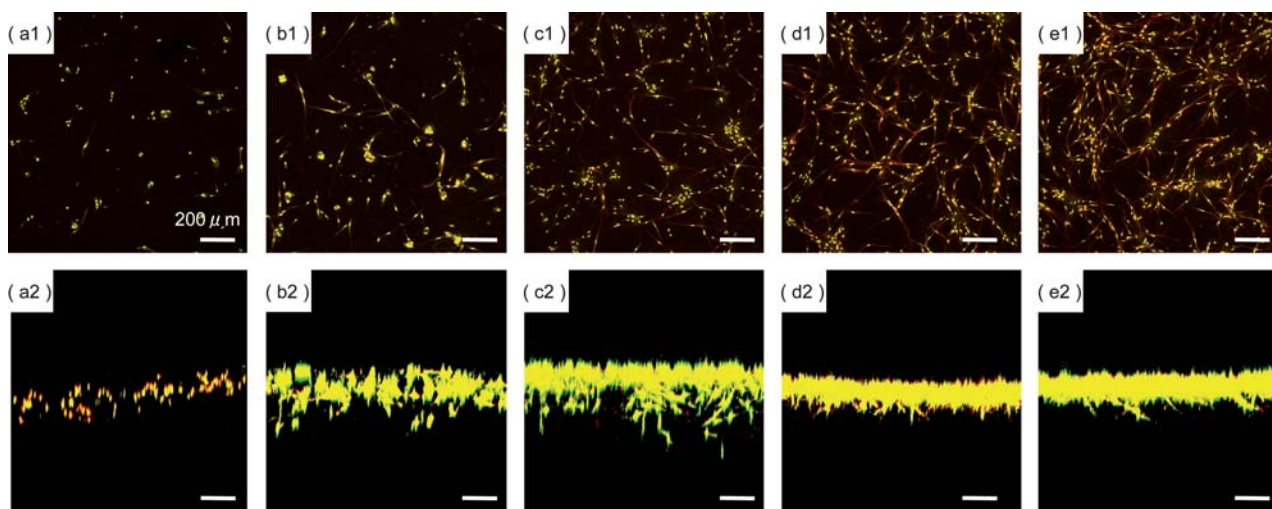


Fig. 4 Projections of 3-D confocal microscopy images of periodontal ligament fibroblasts on each scaffold (a) VEVK9, (b) VEVK9 mixed with vPRG, (c) VEVK9 mixed with vPRG and vPVG, (d) VEVK9 mixed with vYIG and vPVG, (e) VEVK9 mixed with vIKV and vPVG. (a1–e1) Vertical and (a2–e2) horizontal images after three weeks culture. There were significant cell migration into scaffold VEVK9 mixed with vPRG and vPVG. The bars represent 200 μm .

A variety of functionalized peptide scaffolds have been developed and shown a great potential for tissue engineering and regenerative medicine.^{7,8,25} Most of them are functionalized with cell adhesion motifs derived from extracellular matrix proteins. They are responsible for the first interaction between cell and matrix, cell adhesion to promote cell growth included cell migration. But since these functionalized peptide scaffolds are not enzymatically degradable, their ability to promote cell migration is limited. In the nondegradable scaffolds, cells seem to squeeze through the spaces between nanofibers of the scaffolds. As an amoeboid cell migration depends on the mechanical properties of the peptide scaffold, the strategy of using a cell adhesion motif is limited to scaffolds with relatively large pores and soft nanofibers which cells can penetrate. In contrast, enzymatically degradable peptide scaffolds enable a significant increase in cell migration. The peptide scaffolds functionalized with vPVG in Fig. 4 seem to be enzymatically degradable and promoted proteolytic cell migration. The MMP cleavable motif tested here may be useful to functionalize most of self-assembling peptides without considering the mechanical properties. Also, when combined with a cell adhesion motif in varying proportions, it would be possible to design suitable peptide scaffolds for specific applications. For example, these peptide scaffolds may be useful as alternatives for naturally occurring extracellular matrix derived materials such as fibrin or collagen, which require difficult purification procedures and carry the risks of immunogenicity and disease transmission.

3.4 Effect of mechanical properties of peptide scaffolds on cell growth

Fig. 6 shows the Young's modulus, a measure of mechanical stiffness, of each peptide scaffold without cells. The peptide scaffold VEVK9 and the functionalized scaffolds containing VEVK9 were less stiff than those containing VEVK12. When VEVK9 was mixed with functionalized peptides, there was a tendency to increase stiffness of the peptide scaffolds.

Self-assembling peptides like VEVK9 and VEVK12 form a β -sheet filament structure stabilized by hydrogen bonds and ionic interactions between charged side chains. These filaments assemble in salted water through a charge screening effect. Previous studies have shown that scaffold stiffness can vary with peptide length.^{11–15} It appears that the large number of hydrogen and ionic bonds between amino acids in the self-assembly of VEVK12 form higher strength nanofibers than VEVK9. However, the role of peptide length is complex, and this conclusion would need to be tested with shorter or longer peptides.

Functionalized peptides of RADA16-I with a variety of biologically active motifs have been shown to significantly promote cell attachment, proliferation, migration and differentiation.^{7,8} However it is still unknown how the functionalized peptides are incorporated into the nanofibers and how they affect cell activities. Notably, some of the functionalized peptides have a tendency to undergo very weak self-assembly to form soft hydrogels.^{8,25} Therefore these functionalized peptides were thought to stimulate cell activities not only by the biologically active motifs, but also by the change in scaffold stiffness. The findings from this study show that the changes in cell activity on

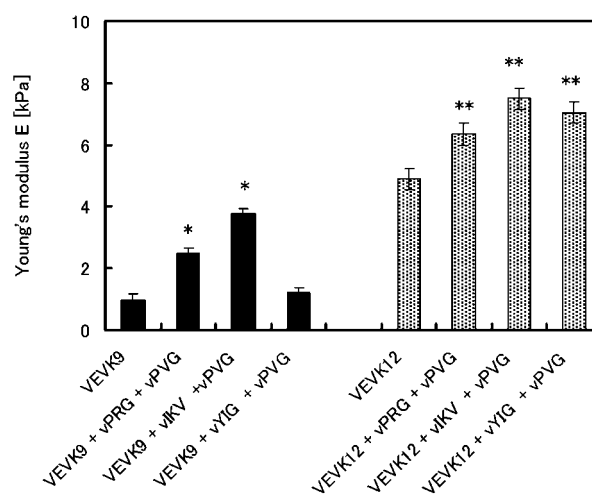


Fig. 6 Mechanical stiffness of cell-free peptide scaffolds. Peptide scaffolds VEVK9 mixed with functionalized peptides except vYIG and vPVG are significantly stiffer than VEVK9 alone (* $P < 0.05$ vs. VEVK9). Peptide scaffolds VEVK12 mixed with all functionalized peptides tested here are significantly stiffer than VEVK12 alone (** $P < 0.05$ vs. VEVK12).

the functionalized peptides tested here may be due to the biologically active motifs and do not simply correlate with the stiffness of the scaffold. In the peptide scaffolds VEVK9, VEVK9 mixed with vPRG and vPVG, and VEVK9 mixed with vIKV and vPVG, cell proliferation significantly increased with an increase in the higher stiffness. However, despite the fact that VEVK9 mixed with vYIG and vPVG is as soft as VEVK9, cell proliferation significantly increased on the scaffold (Fig. 3, Fig. 6). Cell migration significantly increased in VEVK9 mixed with vPRG and vPVG. In the other scaffolds, VEVK9 mixed with vIKV and vPVG, and VEVK9 mixed with vYIG and vPVG, the same degree of 3D cell migration was observed in spite of the different level of stiffness (Fig. 4, Fig. 6). Meanwhile, the biologically active motifs incorporated into the self-assembling peptide seem to play their function in the scaffolds. It is clear in Fig. 3 that vPRG, vIKV and vYIG, which are functionalized with cell adhesion motifs, affected cell adhesion on the peptide scaffolds and significantly increased cell numbers after three weeks culture. It is also clear in Fig. 4 that vPVG, which is functionalized with MMP cleavable site, affected cell migration.

The functionalization of self-assembling peptide with biologically active motifs seems to be an effective way to develop fully synthetic biological material which activate cells in an appropriate manner.

3.5 Scaffold material for periodontal tissue repair

We here demonstrated that fully designer peptide scaffolds significantly accelerated periodontal ligament proliferation and migration. This is a significant finding that these simple motifs could have a drastic influence on the fibroblasts' activities. It is much easier and less expensive to produce the peptide scaffold than to use complex and expensive soluble factors that show similar cell behavior. These peptide scaffolds have potential value as scaffold materials for tissue engineering and regenerative medicine, for example periodontal tissue reconstruction.

The periodontium, the tooth support apparatus, consists of four tissues, gingival, periodontal ligament, cementum and alveolar bone. The diverse composition of the periodontium makes periodontal wound healing a complex process because of the interaction between hard and soft connective tissues, implying the selective repopulation of the root surface by cells capable of reforming the cellular and extracellular components of new periodontal ligament, cementum and alveolar bone.³² Guided tissue regeneration is often discussed as a method for periodontal tissue reconstruction, which could restrict the repopulation of a defect to gingival tissue, providing space and a favorable niche to maximize periodontal ligament fibroblasts, cementoblasts and osteoblasts to migrate selectively, proliferate and differentiate.^{33–35} The periodontium is also known as a highly vascularized tissue. The blood supply is important not only for nutrition of newly engineered tissues, but also to maintain the local homeostasis and adequate host defence by transporting cells and defensins to the gingival crevice.³⁶

For successful clinical use of in periodontal tissue reconstruction, functionalized peptide scaffolds would be required to allow selective cell repopulations and promote angiogenesis. It has been previously reported that the peptide scaffold functionalized with RGD could control osteoblasts' activities by changing the concentration of the functionalized peptide.⁸ It also has been reported that laminin has specific cell adhesion properties, which favored adhesion by periodontal ligament fibroblasts and osteoblasts over adhesion by gingival fibroblasts.^{28,29} For angiogenesis, the above-mentioned peptide scaffold functionalized with RGD was also shown to promote endothelial cell growth.²⁵ Furthermore the functionalized peptide vPVG tested here seems to be effective for endothelial cell proteolytic migration. A variety of functionalizations of the self-assembling peptides will enable optimization of the scaffolding materials for many uses, included periodontal tissue reconstruction. We will assess the efficacy of these peptide scaffolds using an animal experimental model.

Conclusions

We have developed and evaluated self-assembling peptides VEVK9, VEVK12 and functionalized designer self-assembling peptide scaffolds with cell adhesion motifs and MMP cleavage sites. In our study these functionalized peptide scaffolds have been shown to significantly enhance periodontal ligament fibroblast proliferation and migration in 3D cell culture independent of scaffold stiffness. Thus these designer scaffolds will be widely useful in tissue engineering and regenerative medicine.

Acknowledgements

We gratefully acknowledge a support of Olympus Corporation for this study. SZ was supported in part by grant from NIBIB BRP Grant EB003805 to MIT CBE.

Notes and references

1 S. Zhang, T. C. Holmes, C. Lockshin and A. Rich, *Proc. Natl. Acad. Sci. U. S. A.*, 1993, **90**, 3334–3338.

- 2 S. Zhang, T. C. Holmes, C. M. DiPersio, R. O. Hynes, X. Su and A. Rich, *Biomaterials*, 1995, **16**, 1385–1393.
- 3 S. Koutsopoulos, L. D. Unsworth, Y. Nagai and S. Zhang, *Proc. Natl. Acad. Sci. U. S. A.*, 2009, **106**, 4623–4628.
- 4 Y. Yang, U. Khoe, X. Wang, A. Horii, H. Yokoi and S. Zhang, *Nano Today*, 2009, **4**, 193–210.
- 5 H. Yokoi, T. Kinoshita and S. Zhang, *Proc. Natl. Acad. Sci. U. S. A.*, 2005, **102**, 8414–8419.
- 6 R. G. Ellis-Behnke, Y. X. Liang, S. W. You, D. Tay and S. Zhang, *Proc. Natl. Acad. Sci. U. S. A.*, 2006, **103**, 5054–5059.
- 7 R. G. Ellis-Behnke, Y. X. Liang, D. Tay, P. W. F. Kau, G. E. Schneider, S. Zhang, W. Wu and K. F. So, *Nanomed.: Nanotechnol., Biol. Med.*, 2006, **2**, 207–215.
- 8 A. Horii, X. M. Wang, F. Gelain and S. Zhang, *PLoS One*, 2007, **2**, e190.
- 9 F. Gelain, D. Bottai, A. Vescovi and S. Zhang, *PLoS One*, 2006, **1**, e119–11.
- 10 J. Kisiday, M. Jin, B. Kurz, H. Hung, C. E. Semino, S. Zhang and A. J. Grodzinsky, *Proc. Natl. Acad. Sci. U. S. A.*, 2002, **99**, 9996–10001.
- 11 E. J. Leon, N. Verma, S. Zhang, D. A. Lauffenburger and R. D. Kamm, *J. Biomater. Sci., Polym. Ed.*, 1998, **9**, 297–312.
- 12 M. Caplan, P. Moore, S. Zhang, R. D. Kamm and D. A. Lauffenburger, *Biomacromolecules*, 2000, **1**, 627–631.
- 13 M. Caplan, E. M. Schwartzfarb, S. Zhang, R. D. Kamm and D. A. Lauffenburger, *Biomaterials*, 2002, **23**, 219–227.
- 14 M. Caplan, E. M. Schwartzfarb, S. Zhang, R. D. Kamm and D. A. Lauffenburger, *J. Biomater. Sci., Polym. Ed.*, 2002, **13**, 225–236.
- 15 D. Marini, W. M. Hwang, D. A. Lauffenburger, S. Zhang and R. D. Kamm, *Nano Lett.*, 2002, **2**, 295–299.
- 16 W. M. Hwang, D. Marini, R. D. Kamm and S. Zhang, *J. Chem. Phys.*, 2003, **118**, 389–397.
- 17 M. P. Lutolf, J. L. Lauer-Fields, H. G. Schmoekel, A. T. Metters, F. E. Weber and G. B. Fields, *Proc. Natl. Acad. Sci. U. S. A.*, 2003, **100**, 5413–5418.
- 18 H. W. Jun, V. Yuwono, S. E. Paramonov and J. D. Hartgerink, *Adv. Mater.*, 2005, **17**, 2612–2617.
- 19 Y. Chau, Y. Luo, A. C. Y. Cheung, Y. Nagai, S. Zhang, J. B. Kobler, S. M. Zeitel and R. S. Langer, *Biomaterials*, 2008, **29**, 1713–1719.
- 20 B. Law, R. Weissleder and C. H. Tung, *Biomacromolecules*, 2006, **7**, 1261–1265.
- 21 M. P. Lutolf, F. E. Weber, H. G. Schmoekel, J. C. Schense, T. Kohler, R. Muller and J. A. Hubbell, *Nat. Biotechnol.*, 2003, **21**, 513–518.
- 22 D. Seliktar, A. H. Zisch, M. P. Lutolf, J. L. Wrana and J. A. Hubbell, *J. Biomed. Mater. Res.*, 2004, **68a**, 704–716.
- 23 C. B. Bahney, C. W. Hsu, J. West and B. Johnstone, presented in part at Society for Biomaterials 2009 Annual meeting and exposition, San Antonio, April, 2009.
- 24 C. A. DeForest, E. A. Sims, B. D. Polizzotti and K. S. Anseth, presented in part at Society for Biomaterials 2009 Annual meeting and exposition, San Antonio, April, 2009.
- 25 X. M. Wang, A. Horii and S. Zhang, *Soft Matter*, 2008, **4**, 2388–2395.
- 26 B. E. Turk, L. L. Huang, E. T. Piro and L. C. Cantley, *Nat. Biotechnol.*, 2001, **19**, 661–667.
- 27 J. L. Hutter and J. Bechhoefer, *Rev. Sci. Instrum.*, 1993, **64**, 1868–1873.
- 28 A. A. Palaiologou, R. A. Yukna, R. Moses and T. E. Lallier, *J. Periodontol.*, 2001, **72**, 798–807.
- 29 C. Giannopoulou and G. Cimasoni, *J. Dent. Res.*, 1996, **75**, 895–902.
- 30 E. Tsuruga, K. Irie and T. Yajima, *J. Dent. Res.*, 2007, **86**(4), 352–356.
- 31 J. Xu, D. Rodrigues, E. Petitelec, J. J. Kim, M. Hangai, S. M. Yuen, G. E. Davis and P. C. Brooks, *J. Cell Biol.*, 2001, **154**, 1069–1079.
- 32 M. Taba Jr, Q. Jin, J. V. Sugai and W. V. Giannobile, *Orthodont. Craniofacial Res.*, 2005, **8**, 292–302.
- 33 S. Nyman, J. Lindhe, T. Karring and H. Rylander, *J. Clin. Periodontol.*, 1982, **9**, 290–296.
- 34 J. Lindhe, R. Pontoriero, T. Verglundh and M. Araujo, *J. Clin. Periodontol.*, 1995, **22**, 276–83.
- 35 J. B. Park, M. Matsuura, K. Y. Han, O. Norderyd, W. L. Lin, R. I. Genco and M. I. Cho, *J. Periodontol.*, 1995, **66**, 462–77.
- 36 M. S. McKay, E. Olson, M. A. Hesla, A. Panyutich, T. Ganz and S. Perkins, *Oral Microbiol. Immunol.*, 1999, **14**, 190–193.